Silica and alumina impregnated with dimethylformamide solutions of molybdophosphoric or tungstophosphoric acids for hydrotreatment reactions

Alain Rives [a], Edmond Payen [a], Robert Hubaut [a], Patricia Vázquez [b], Luis Pizzio [b], Carmen Cáceres [b] and Mirta Blanco [b,*]

[a] *Laboratoire de Catalyse, UPRESA 8010, Université des Sciences et Technologies de Lille, 59655 Villeneuve d'Ascq Cedex, France*
[b] *Centro de Investigación y Desarrollo en Procesos Catalíticos (CINDECA), UNLP, CONICET, 47 No. 257, 1900 La Plata, Argentina*
E-mail: hds@dalton.quimica.unlp.edu.ar

Received 12 June 2000; accepted 6 November 2000

Heteropolyacid (HPA) based catalysts were prepared by impregnation of silica and alumina with dimethylformamide solutions of molybdophosphoric and tungstophosphoric acids. This solvent allows the preservation of the Keggin unit during the impregnation independently of the nature of the support. Ni-promoted catalysts were prepared by impregnation with nickel nitrate solutions of the supported HPA. The stronger interaction of the HPA with alumina than with silica allows a better dispersion of the polyoxometallate species on the former one whereas the formation of bulk oxides is observed on silica. The performance of these HPA–Ni/support catalysts for hydrodenitrogenation and hydrodesulfurization reactions is related to the precursor–support interaction.

KEY WORDS: supported catalysts; heteropolyacids; silica; alumina; hydrodenitrogenation; hydrodesulfurization

1. Introduction

The development of new Co–Mo–Al_2O_3 and Ni–Mo–Al_2O_3 catalysts has been carried out by the need to produce clean fuels, based on the pressing requirement for environmental protection. Some of these commercial hydrodesulfurization catalysts contain phosphorus as additive. They are obtained by sulfidation of an oxidic precursor, which is prepared by impregnation of an alumina support with solutions containing the components to be deposited. The most commonly used method of preparation is based on the dissolution of ammonium heptamolybdate (AHM) in presence of phosphoric acid [1]. The presence of the diphosphopentamolybdate anion $[P_2Mo_5O_{23}]^{6-}$ in this conventional impregnating solution has been proposed [2]. The use of Keggin acids or salts ($H_3PMo_{12}O_{40}$, $Co_{3/2}PMo_{12}O_{40}$ or $Ni_{3/2}PMo_{12}O_{40}$) [3–6] or Anderson salts ($[H_6XY_6O_{24}]^{x-}$ with X = Co or Ni and Y = Mo or W) [7–9] as starting materials has also been reported. It has been shown that alumina is not suitable as a support because it probably decomposes the heteropolyacid (HPA) primary structure (the Keggin unit) [10] whereas silica has a less destabilizing effect [11]. All these studies have been performed using aqueous solutions of the starting heteropolyanions, but it is well known that the stability of the heteropolyanions is strongly dependent on the pH [12]. We have decided to study the impregnation using DMF solution as it has been shown that this solvent may stabilize the Keggin structure [13]. In this paper we report the preparation of Ni–Mo–P and Ni–W–P based catalysts using silica or alumina as support. Comparisons were carried out through physical characterizations of the impregnating solutions as well as through the characterizations of the oxidic precursors at each step of their preparations. These oxidic precursors were then sulfided and the activities of these catalysts were evaluated in hydrodesulfurization (HDS) and hydrodenitrogenation (HDN) of a mixture of cyclohexane–pyridine–thiophene. The efficiencies of these catalysts were compared and discussed in reference to the different nature of the species present on the support surface.

* To whom correspondence should be addressed.

2. Experimental

2.1. Sample preparation

The impregnating solutions were prepared using commercial pure reagent grade products without further purification, i.e., molybdophosphoric acid (MPA), $H_3PMo_{12}O_{40}$, from Merck, tungstophosphoric acid (TPA), $H_3PW_{12}O_{40}$, from BDH or nickel nitrate from Fluka in dimethylformamide (DMF) from Carlo-Erba as solvent.

Commercial γ-alumina spheralite (surface area 282 m^2/g, pore volume 0.42 cm^3/g, mean pore diameter 4.8 nm) and silica Ralt-Chemie (surface area 281 m^2/g, pore volume 0.84 cm^3/g, mean pore diameter 8.5 nm) were used as supports.

The catalysts were prepared by the pore filling method using a two-step impregnation according to the procedure previously described [14]. First, MPA or TPA acids were impregnated on the alumina (silica) from solutions in DMF; in the second step, after drying at 70 °C for 48 h, the catalysts were impregnated with DMF solution of nickel nitrate.

1011-372X/01/0200-0193$19.50/0

Solids obtained in this way were dried at room temperature during 24 h and then calcined at 350 °C during 1 h. The nomenclature of the samples will be A–Ni/S, where A is the nature of the HPA (MPA or TPA) and S is the nature of the support (Al_2O_3 or SiO_2). Ni is omitted to designate the non-promoted samples.

2.2. Physical characterizations

UV-visible spectra of the solutions before and after the contact with both tested supports and in excess of solution were recorded in the 200–400 nm range. A UV-visible double-beam Varian Super Scan 3 spectrophotometer, quartz cells of 0.5 mm optical path and water as reference were used.

Quantitative analysis of the prepared solids was obtained by atomic absorption with an IL 457 spectrometer after dissolution in an acid solution. Their characterizations were performed on the solids finely ground in a mortar.

Specific surface area, mean pore diameter and pore volume were determined from the N_2 adsorption–desorption isotherms at 77 K made in a Micromeritics Accusorb 2100E equipment. The samples were previously degassed at 100 °C for 1 h.

UV-visible diffuse reflectance spectra (DRS) of the solids were obtained in the 200–600 nm spectral range by means of a Varian Super Scan 3 spectrometer equipped with a diffuse reflectance accessory. The sample was compacted in a Teflon sample holder and was covered with a quartz circular window to obtain a sample thickness of 2 mm. Spectra of non-promoted and promoted oxidic solids were scanned against a pure support (alumina or silica) background.

X-ray diffraction (XRD) patterns were carried out with a Philips PW-1714 diffractometer equipped with a Cu X-ray tube and a Ni filter.

A Bruker IFS 66 equipment with the KBr pellet method was used to obtain the infrared (FTIR) spectra. Bulk acids, sodium salt of 11-tungstophosphate anion (lacunar phase), dried at 70 °C, and silica-supported solids, before and after the impregnation with nickel, were examined in the spectral range of 400–1500 cm^{-1}. The lacunar phase was prepared, according to [15], from a TPA aqueous solution alkalized and evaporated to dryness.

Laser Raman spectroscopy (LRS) of the solids in room air was carried out using a Raman microprobe (XY from Dilor), equipped with a photodiode array. The exciting light source was an Ar^+ laser emitting the 514.5 nm line with a power at the sample of 1 mW.

Nuclear magnetic resonance spectroscopy (NMR) of the solid samples was carried out by means of a Bruker MLS-300 equipment, using 5 μs pulses, a repetition time of 3 s and working at a frequency of 121.496 MHz for ^{31}P at room temperature. Phosphoric acid 85% was used as external reference. The spin rate was 2.1 kHz and several hundred responses were collected.

X-ray photoelectron spectra (XPS) were recorded by using an AEI ES200B spectrometer equipped with an aluminium X-ray source working at 300 W. The solids were pressed on an indium foil. The binding energies (BE) of the various elements were referred to the Al 2p peak of the support at 74.4 eV and to the Si 2p at 103.5 eV, respectively, for the alumina- and the silica-based solids.

Temperature-programmed reduction (TPR) experiments were performed in the range 20–1000 °C; the temperature was increased at 10 °C/min in a H_2 flow of 90 cm^3/min.

2.3. Catalytic activity

The activity measurements in HDS and HDN reactions were accomplished on the ground catalysts (between 60 and 100 mesh). A fixed bed reactor working at 3 MPa, 280°C, with a H_2/HC molar ratio 5 and LHSV = 53 h^{-1} was used. The liquid feed was a mixture of cyclohexane–pyridine (2000 ppm N)–thiophene (6000 ppm S). The catalysts (1.2 g) were presulfurized *in situ* at 280 °C and 1.8 MPa for 1 h in a flow of H_2S/H_2 (10 : 90). The reactants and reaction products were analyzed by gas chromatography (ionization flame detector) with a column packed with 4% Carbowax 90M + 0.8% KOH on Graphpac GB, using a programmed temperature increase between 90 and 170 °C and nitrogen as carrier. The conversion was calculated after 4 h under reaction as the ratio of thiophene or pyridine consumption to the initial quantity.

3. Results and discussion

3.1. The impregnating solution

Previously to the preparation of the catalysts, a study of the behavior of the TPA and MPA solutions in DMF was performed, in order to verify that the Keggin structure of the heteropolyanions is preserved when it is dissolved in DMF. With this purpose, the UV-visible spectra of the solutions as a function of time, before and after the contact with both tested supports, were recorded (figure 1 (I) and (II)). The spectrum (b) of the initial MPA solution (120 mg Mo/ml), 72 h after its preparation, and the solutions after different contact times with alumina (c) and silica (d) present the charge-transfer band with maximum at 315 nm, assigned to $[PMo_{12}O_{40}]^{3-}$ anion [16]. The broad band observed below 240 nm is due to DMF, as it can be seen in the spectrum (a) of the solvent shown in figure 1(I). A similar behavior was observed for TPA solutions. The characteristic charge-transfer band of $[PW_{12}O_{40}]^{3-}$ anion with a maximum at 265 nm [17] can be seen in all the spectra (figure 1(II)). For both MPA and TPA solutions, the decrease of the band intensity in function of time, more outstanding when using alumina, is due to the decrease of HPA solution concentration, as adsorption proceeds. So, the heteropoly structures are preserved by means of dissolution in DMF, as it was expected from our previous ^{31}P NMR study [14,18]. Besides, this demonstrates that UV-visible spectroscopy can be a good tool for the species characterization in these systems in solution.

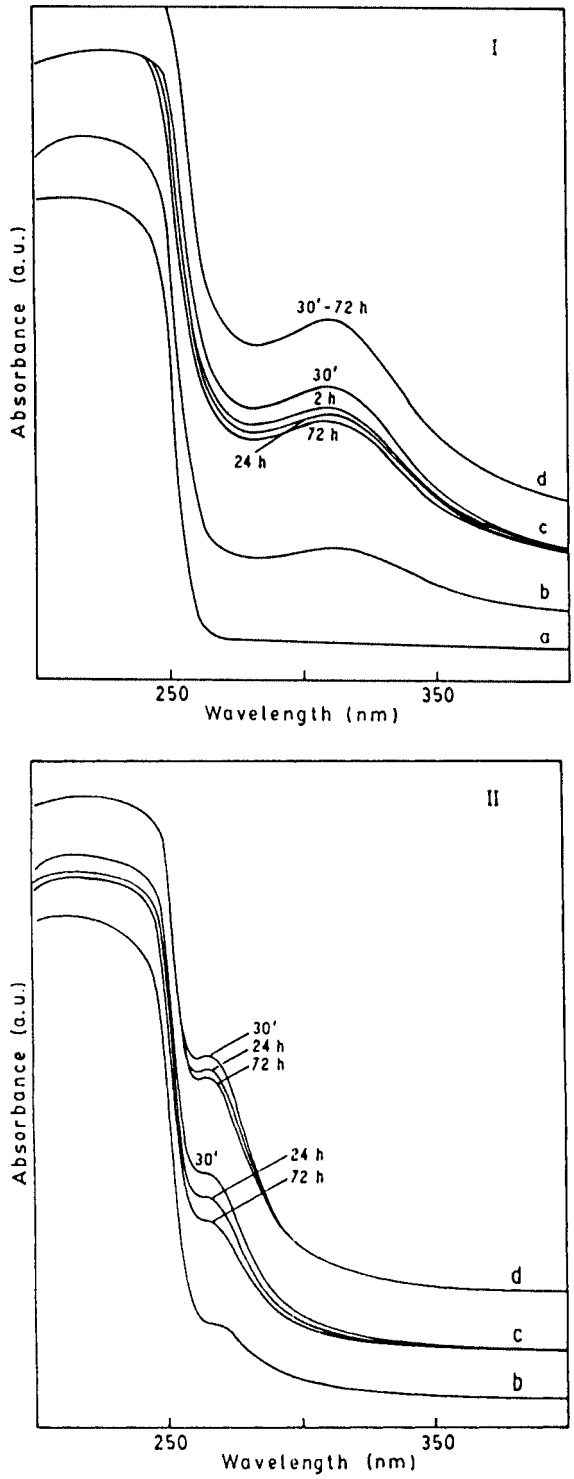

Figure 1. UV-visible spectra of: (I) DMF solvent (a), MPA solutions before (b) and after the contact with alumina (c) or silica (d); (II) idem for TPA solutions.

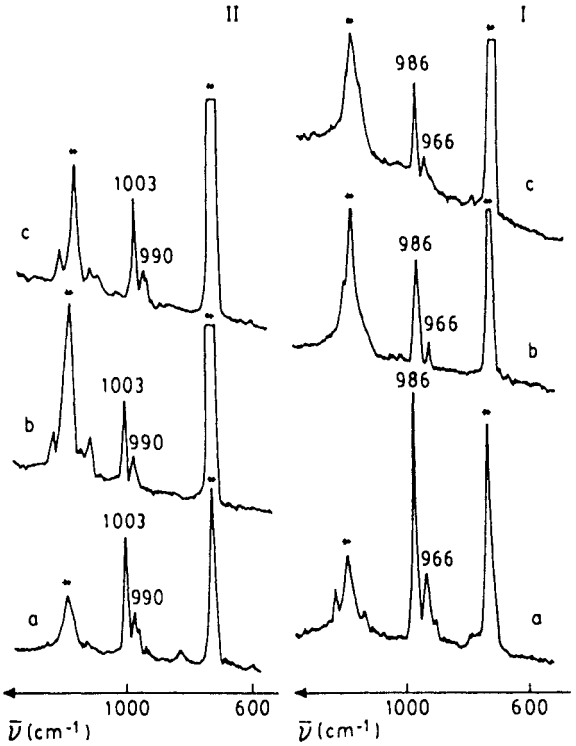

Figure 2. Raman spectra of: (I) MPA solutions before (a) and after impregnation of alumina (b) or silica (c); (II) idem for TPA (* lines of DMF).

The preservation of the Keggin structure by means of dissolution in DMF is also confirmed by laser Raman spectroscopy, as seen in figure 2 (I) and (II) spectra (a), which show the Raman spectra of the DMF solutions before the impregnation. They characterize, by reference to [13], the presence of MPA and TPA in DMF, respectively. So, the stabilizing effect of DMF as solvent compared to water [18] for preparing the impregnating solutions is verified. Indeed Fournier et al. [13] suggested that the model of anion–cation aggregates allows the behavior of the heteropolyacids in DMF solutions to be explained. They have also proposed that there is no solvation of the anions dissolved in DMF but the Keggin anions interact with the protonated solvent ($DMFH^+$ entity). The aggregate formation should favor the Keggin structure preservation. After impregnation, using either support, the Raman lines of MPA (figure 2(I), spectra (b)–(c)) and TPA (figure 2(II), spectra (b)–(c)) are still observed in agreement with the above-mentioned UV study whereas no features of their decomposition products are evidenced. This shows that the Keggin structure is not modified during the introduction of the support in the solution.

On the other hand, the greater absorbance decrease of the UV bands, when the contact time of the solution with the alumina increases, shows that the HPA are adsorbed in a greater amount on alumina as compared with silica. This is also an indication that the samples prepared using silica will contain a greater HPA concentration in weak interaction with the support.

3.2. The supported solids

3.2.1. The wet and dried Mo(W)/support solids

Figure 3 (I) and (II) shows the DRS spectra of the catalysts prepared from MPA and TPA, respectively. Spectra of bulk acids and sodium tungstate or molybdate are also shown. Bulk acids present a band at 220 nm and another

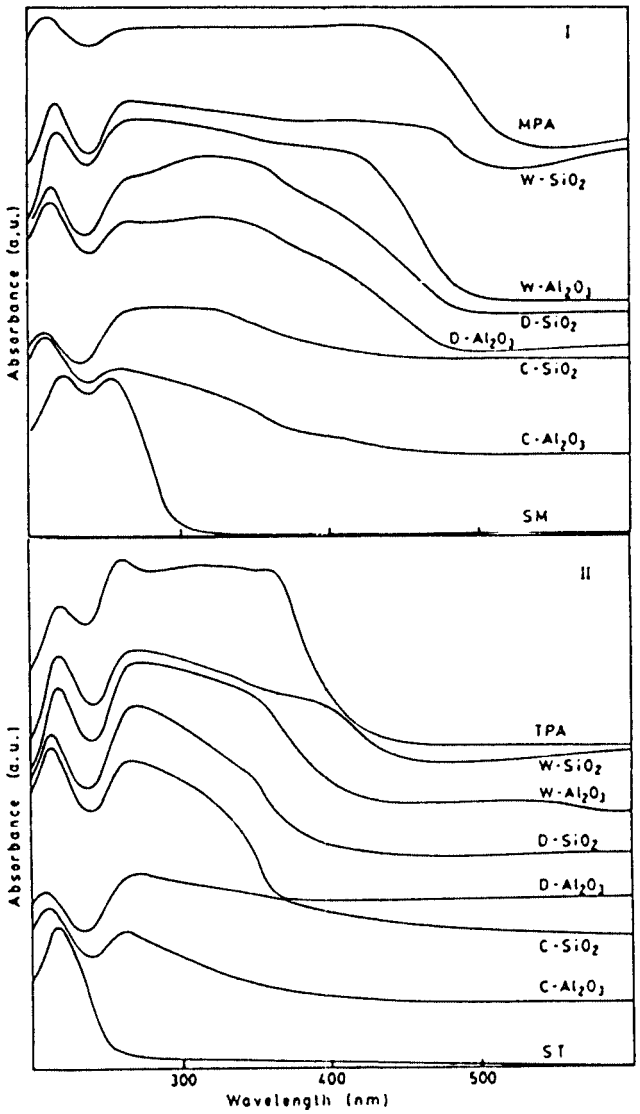

Figure 3. Diffuse reflectance spectra of: (I) bulk MPA; wet (W), dried (D) and calcined (C) MPA catalysts and sodium molybdate (SM); (II) idem for TPA and sodium tungstate (ST).

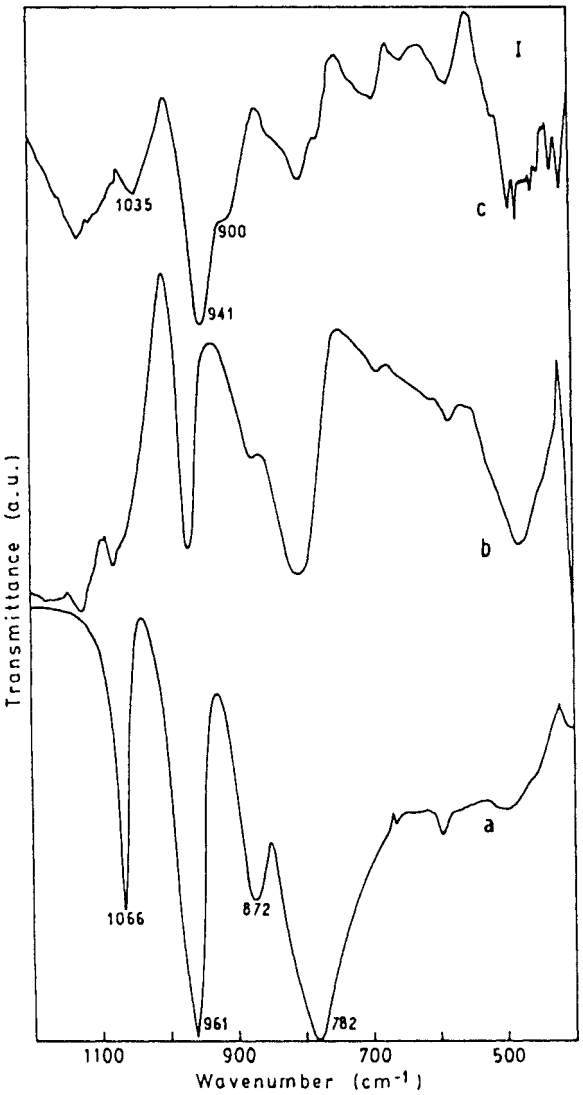

Figure 4. Fourier transformed infrared spectra of: (I) bulk MPA (a), MPA catalyst supported on silica before (b) and after (c) the impregnation with nickel; (II) idem for TPA and sodium salt of $[PW_{11}O_{39}]^{7-}$ ion (d).

broad band from 260 nm up to about 500 nm for MPA and 450 nm for TPA. It can be seen that all wet samples show the characteristic band of the Keggin structure. The spectra of dried silica samples show the bands corresponding to the undegraded species and spectra of dried alumina ones show an absorbance increase of the band at 220 nm. As can be seen in figure 3, the DRS band maxima of sodium molybdate are placed at 220 and 260 nm and the spectrum of sodium tungstate shows a band with maximum at around 220 nm. More or less polymerized polymolybdates also show bands in the 220 and 350 nm spectral region [19]. All of them show absorbance at the wavelengths where dried alumina-supported catalysts spectra exhibit the absorbance increase. This can be attributed to partial structure transformation, giving rise to monomeric and/or polymeric isopoly species.

The FTIR spectrum of bulk $H_3PMo_{12}O_{40}$ (figure 4(I), (a)) shows bands at 1066, 961, 872 and 782 cm^{-1}, in agreement with those reported in the literature for this acid [20,21]. The spectrum (b) (figure 4(I)) of the dried MPA/SiO_2 exhibits the same main bands as bulk MPA. Similarly, regarding the FTIR spectrum of bulk $H_3PW_{12}O_{40}$ (figure 4(II), (a)), bands at 1081, 982, 888, 793, 595 cm^{-1} are observed, in agreement with literature data [21]. The spectrum (b) of TPA on silica exhibits the main bands of the $[PW_{12}O_{40}]^{3-}$ heteropolyanion. However, some variations of intensity are observed for the line in the high-frequency range which should be ascribed to the standard support subtraction used to obtain the spectra, since the strongest absorption band of the silica is in this spectral range [22]. No information could be obtained for the alumina-based samples due to the intense absorption of the support.

The wet alumina- and silica-based solids have therefore been analyzed by LRS. However, the Raman spectra reported in figure 5 should be considered as characteristic of partially dried solids, as the characteristic lines of the DMF

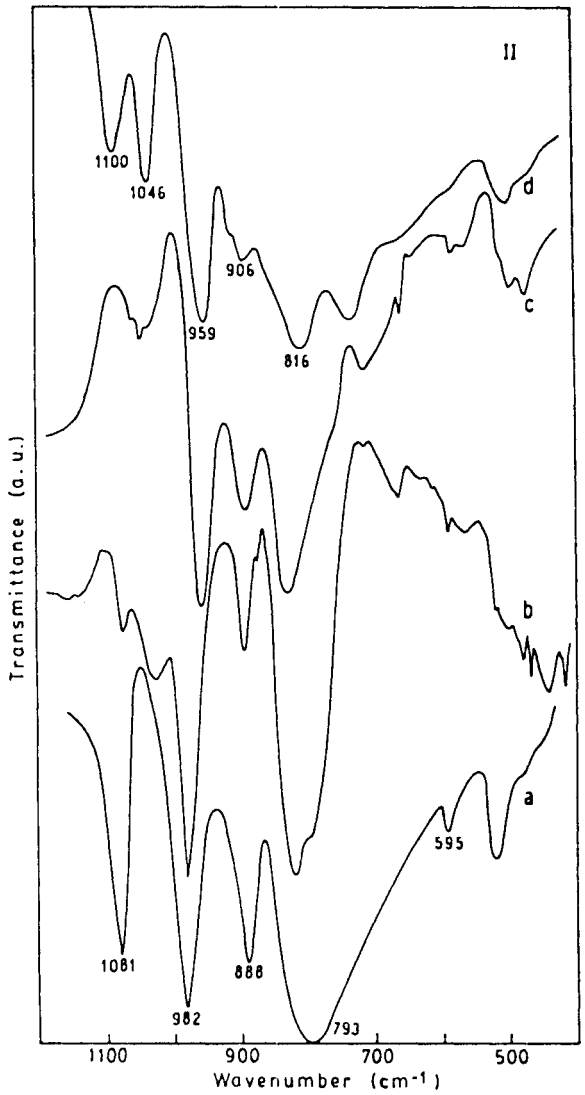

Figure 4. (Continued.)

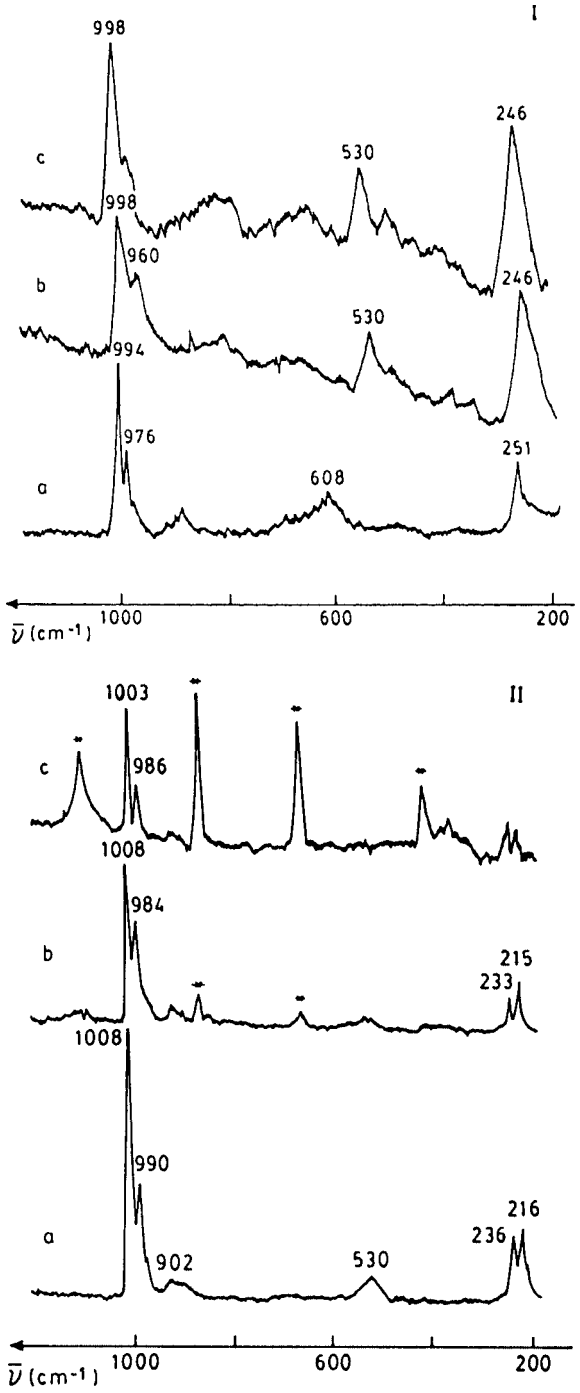

Figure 5. Raman spectra of wet oxidic precursor: (I) bulk MPA (a), MPA/Al_2O_3 (b) and MPA/SiO_2 (c); (II) idem for TPA.

are always very weak or not observed. This should be assigned to the irradiation of the laser beam in spite of the very low power used. With both supports, the main Raman lines of the MPA and TPA in their solid form are observed at, respectively, 994 and 251 cm^{-1} and 1008, 990 and 236 cm^{-1}, which were similar to those reported in the literature [23,24]. Even though small variations are observed for the supported MPA (line at 530 cm^{-1}) that could be ascribed to a small partial degradation of the MPA, we may consider that independently from the HPA and the carrier, the primary structure is preserved during impregnation.

The dried samples have also been characterized by ^{31}P nuclear magnetic resonance spectroscopy. The silica-supported TPA sample presents the most intense line at -14.4 ppm and a small shoulder at -15 ppm (figure 6). These were ascribed by Lefebvre [25] to the heteropolyanion in slight interaction with the surface and to TPA without interaction, respectively. A similar assignment can be made to the lines at -3.2 and -3.9 ppm, respectively, observed in the spectrum of MPA on silica [26]. So, it can be stated that the heteropolyanions in slight interaction with the surface when supported on silica are the main species. MPA supported on alumina presents a broad line with a maximum at -4.2 ppm, which may be assigned to the undegraded $[PMo_{12}O_{40}]^{3-}$ heteropolyanion, although the signal enlargement and the small upfield shift can be attributed to a greater interaction than on silica. For TPA supported on alumina two lines at -13.0 and -15.1 ppm are observed. The latter peak corresponds to the undegraded anion and the former peak can be ascribed to intact Keggin units interacting with surface

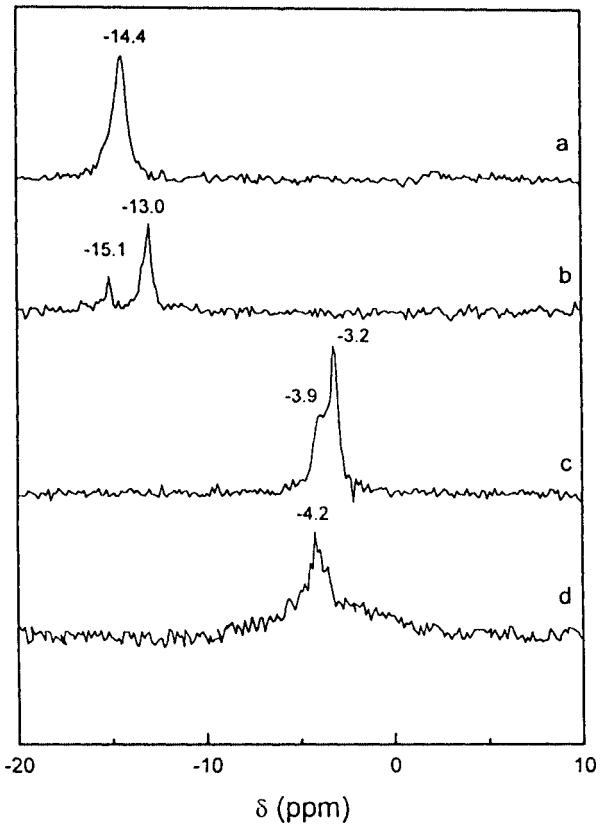

Figure 6. ^{31}P MAS-NMR spectra of TPA/SiO_2 (a), TPA/Al_2O_3 (b), MPA/SiO_2 (c) and MPA/Al_2O_3 (d) dried solids.

hydroxyl groups, as not totally deprotoned species [26,27]. The results obtained proved that the HPA on both supports keep the Keggin structure, previous to nickel impregnation in agreement with the aforementioned Raman results. Also, it can be inferred that the HPA interact more firmly with alumina than with silica.

These results corroborate that the main species present before the impregnation with nickel is the Keggin type HPA not degraded. They are partly in opposition with previous results in which we showed that MPA is preserved on silica [11] but decomposed on the alumina [10] when the solid is prepared with aqueous solution of MPA. The present preservation of the Keggin unit, using either support, should be assigned to the aforementioned stabilizing effect of the solvent (section 3.1).

Table 1 presents the temperature values of the peak maxima in the TPR spectra of the samples before the impregnation with nickel and those of the bulk acids. The latter show a weak signal at low temperatures (330–450 °C) which can be assigned, according to Hodnett and Moffat [28], to loss of lattice oxygen before the decomposition. Very strong signals beyond the decomposition temperature, probably due to the hydrogen reaction with the constituent oxides of the heteropolyacids, are also observed. The supported HPA spectra show two reduction peaks; these peaks are in most cases at higher temperature than those corresponding to bulk HPA. This different evolution of the supported species under the TPR condition may be the result of the interaction of the heteropolyacids with the supports. Moreover, the maxima are found at higher temperature when MPA or TPA are supported on alumina, in accordance with the higher acid amount interacting with the support compared to silica. This is due to a greater interaction of the species with the alumina.

Table 1
Maximum temperatures in TPR spectra of oxidic non-promoted solids.

MPA/SiO_2	MPA/Al_2O_3	MPA	TPA/SiO_2	TPA/Al_2O_3	TPA
TPR peak maxima[a] (°C)					
400m	436m	330w	532w	533w	452w
		522s			574w
		550vs			
		604w			
760m	825m	793vs	852s	882m	750vs

[a] vs: very strong, s: strong, m: medium, w: weak.

Table 2
Metal concentrations of the catalysts.

Catalyst	Mo or W (wt%)	Ni (wt%)	Ni/(Ni + Mo(W))
$MPA–Ni/SiO_2$	10.0	2.8	0.31
$MPA–Ni/Al_2O_3$	10.8	2.2	0.25
$TPA–Ni/SiO_2$	17.2	2.2	0.26
$TPA–Ni/Al_2O_3$	17.2	2.8	0.31

Table 3
Textural properties of the catalysts.

Catalyst	Specific surface area (m^2/g)	Mean pore diameter (nm)	Pore volume (cm^3/g)
$MPA–Ni/SiO_2$	243	7.6	0.76
$TPA–Ni/SiO_2$	192	8.5	0.47
SiO_2	281	8.5	0.84
$MPA–Ni/Al_2O_3$	236	5.2	0.33
$TPA–Ni/Al_2O_3$	196	5.1	0.28
Al_2O_3	282	4.8	0.42

3.2.2. Calcined promoted solids

The experimental Mo, W and Ni contents of the catalysts reported in table 2 show that the Ni/(Ni + Mo(W)) atomic ratio is near the value which gives rise to a maximum in activity, according to [1].

Changes were observed in the textural properties of the solids compared with the bare supports. Specific surface area, mean pore diameters and pore volumes are reported in table 3. A decrease of the surface area and pore volume has been observed in both the silica- and the alumina-supported solids. The deposition of the solute may block pore mouths or may partially fill the pores, principally the smallest pores, and may cause the effects observed mainly for the supported TPA.

The XRD patterns of the catalysts (figure 7) show only the characteristic bands of the supports; neither the diffraction lines of MPA or TPA nor other crystalline phases were

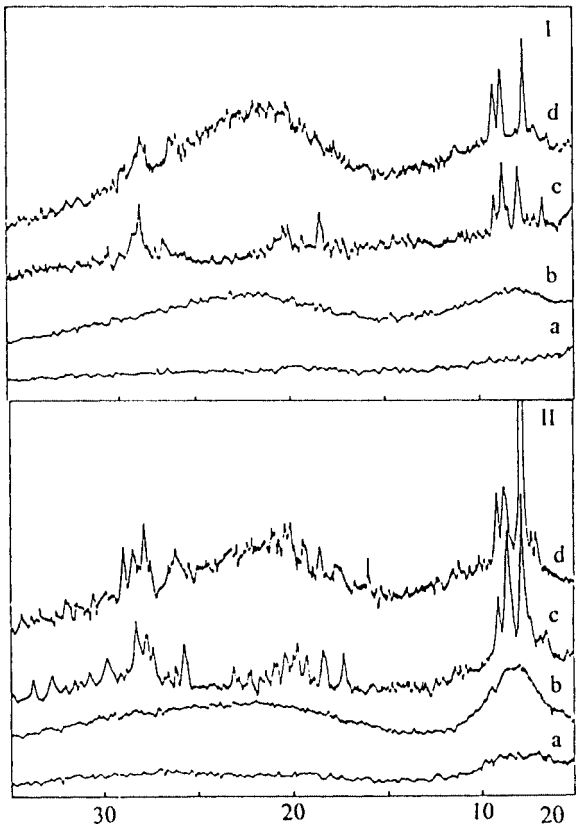

Figure 7. X-ray diffraction patterns of: (I) catalysts MPA–Ni/Al_2O_3 (a) or MPA–Ni/SiO_2 (b) and mechanical mixtures of MPA with alumina (c) or silica (d); (II) idem for TPA.

Table 4
XPS binding energy and atomic ratio of the catalysts.

Sample	BE (eV)[a]		W(Mo)/Al(Si)	
	W 4f or Mo 3d	Ni 2p	Experimental	Nominal
TPA–Ni/SiO_2	35.9	857.6	0.04	0.08
TPA–Ni/Al_2O_3	35.8	857.6	0.08	0.07
MPA–Ni/SiO_2	232.8	856.7	0.02	0.08
MPA–Ni/Al_2O_3	232.9	856.7	0.05	0.07

[a] Referenced to Al 2p at 74.4 eV or Si 2p at 103.5 eV.

observed. In contrast, patterns of mechanical mixtures, prepared with the same metal contents as those of the catalysts, showed the characteristic lines of the HPA in the 2θ ranges: 7°–10° and 27°–29°, as can be seen in patterns (c) and (d) of figure 7 (I) and (II). This indicates that supported species are highly dispersed on the carrier surface and/or present as particles of low crystallinity. They may be adsorbed as separated entities, giving as a result no crystal detection. A similar result was reported by Khozevnikov et al. [29] for TPA on carbon and by Izumi et al. [30] for a silica-supported heteropolyacid.

The dispersion has therefore been characterized by XPS. Table 4 reports the XPS binding energy (BE) as well as the atomic ratio determined by using the integrated intensity ratio of the typical core level (integration of the classical differential semiquantitative XPS equation to infinite sample depth). The comparison has been done with the nominal values, the calculated ratio for the bulk composition. For both supports, the Mo or W BE characterizes Mo^{VI} or W^{VI} in oxidic state, respectively, and the Ni BE characterizes a Ni^{2+} element as in the classical alumina-supported NiMo oxidic precursor [31]. It appears clearly that the oxomolybdate and the oxotungstate phases are well dispersed on alumina support whereas bulk species should be present on silica support.

On the other hand, the UV broad band in DRS spectra is less extended in all calcined samples compared to dried ones (figure 3). This indicates that, using either support, the Keggin phase is at least partially degraded after calcination. Moreover, DRS spectra indicate that the Keggin unit undergoes a greater transformation when supported on alumina than on silica, both at calcination temperature of the samples (350 °C).

The IR spectra of the calcined MPA(TPA)–Ni/SiO_2 catalysts are reported in figure 4. The shift of the band maxima observed in spectra (c), figure 4 (I) and (II), with respect to that in the bulk acids, could be assigned to partial transformation of Keggin anions. If the TPA–Ni/SiO_2 spectrum (II), (c) presents some similarities with that of the lacunary $[PW_{11}O_{39}]^{7-}$ [15,26], whose IR spectrum is reported in figure 4(II), (d), the IR spectrum (I), (c) of the MPA–Ni/SiO_2 supported solid does not accurately correspond to the lacunary $[PMo_{11}O_{39}]^{7-}$ species [15]. As no intense bands are observed in the 700 cm^{-1} spectral range, in which the isopolymolybdates exhibit intense IR absorption bands [32], a total degradation into isopolymolybdate is excluded. This difference could be ascribed to the lower stability of the molybdenum lacunary structure in comparison to the tungsten one. As already mentioned, due to the intense absorption of the support such a characterization is not possible for the alumina-supported solids.

Figure 8 shows the Raman spectra of the calcined oxidic solids. The Raman features of the Keggin unit are no longer observed. The lines characteristic of the bulk MoO_3 (820 and 996 cm^{-1}, spectrum (b)) and WO_3 (788 cm^{-1}, spectrum (d)) oxides are clearly identified, respectively, on the spectra of the MPA and TPA silica-supported solids. However, a close comparison with the spectrum of bulk tungsten oxide indicates a shift of the main line from 808 to 788 cm^{-1} whereas no shift is observed for the molybdenum oxide. This shift has been previously ascribed to the low crystallinity of the oxide or to its interaction with the support [33]. Due to the very high diffusion cross section of the bulk oxide compared to the supported oxoanions, these lines should not be interpreted as the result from the total transformation during calcination of the supported oxometallate species. In fact, broad lines at 986 and 952 cm^{-1} are also observed and attributed, respectively, to a well dispersed polytungstate and polymolybdate species according to literature data [34]. The main line characteristic of the well dispersed polyoxometallates is only identified on alumina, i.e., polytungstate with the main line at 960 cm^{-1} (spectrum (c) in figure 8) and polymolybdate with the main line at 952 cm^{-1}

(spectrum (a) in figure 8). These results are in agreement with the aforementioned preservation of the Keggin unit on the silica carrier, which transforms into bulk oxide during calcination, whereas the better interaction of the HPA with the alumina allows to avoid this transformation. The well described surface oxometallate phase is therefore obtained.

3.2.3. The sulfided catalysts

The catalysts, sulfided at 280 °C in the same conditions used for activity measurements, were characterized by means of temperature-programmed reduction. The patterns recorded exhibit an intense TPR hydrogen consumption peak with maximum at temperatures around 300 °C (table 5). This peak may be attributed, according to literature data, to the reduction of a well dispersed molybdenum (tungsten)–nickel sulfide phase [35,36]. The area of this TPR peak is also reported in table 5.

It can be seen that the silica-supported samples exhibit a less intense peak than the HPA supported on alumina, indicating a small number of reducible sites. This may be due to a better sulfurization of the oxidic phase formed between molybdenum or tungsten and nickel, as a consequence of a weaker interaction of this phase with silica as compared to alumina.

The structure of the active phase of a catalyst greatly depends on the numerous preparative variables and the successive steps involved in their preparation, so the interaction behavior of the oxidic precursors must be reflected on the final catalysts. XPS results indicated that bulk species should be present on the silica surface, nevertheless the silanol groups of silica should play a role in obtaining a fraction of the HPA dispersed and interacting with the surface. As it was previously stated, all characterizations show that the interaction of the precursors is weaker with silica than with alumina. On the other hand, a better sulfurization was confirmed by the measurement of the sulfur content of the sulfurized catalysts by coulometry. The degree of sulfurization was 70–80% of the total amount of molybdenum or tungsten and nickel for silica-supported HPA and only 45–55% for alumina ones.

The HDN and HDS activities, expressed as per cent conversion, of MPA(TPA)–Ni/Al_2O_3(SiO_2) catalysts are reported in table 6. The HDN and HDS activities of the MPA or TPA silica-supported catalysts are higher than those based on alumina. These results are in agreement with an activity mainly related to the interaction between the HPA and the support. Although strong interaction may lead to better dispersed phases, it may also be disadvantageous because it can induce the formation of the type I NiMo(W)S phase. Besides, a less intense interaction can help to the formation of the type II structure, which has been reported as having a

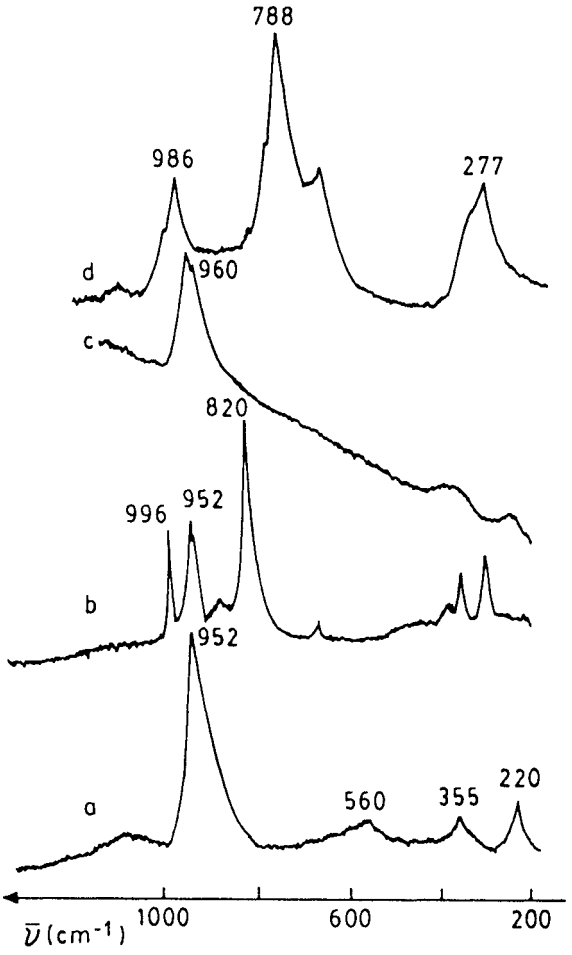

Figure 8. Raman spectra of calcined solids: MPA/Al_2O_3 (a), MPA/SiO_2 (b), TPA/Al_2O_3 (c) and TPA/SiO_2 (d).

Table 5
Maximum temperatures and peak areas in TPR spectra of sulfided catalysts.

MPA–Ni/SiO_2	MPA–Ni/Al_2O_3	TPA–Ni/SiO_2	TPA–Ni/Al_2O_3
	Peak maxima[a] (°C)		
324sh	280s	290s	275s
384s		338sh	
539w	560w	450w	564w
	Peak area[b]		
3.66	12.65	6.15	17.75

[a] s: strong, w: weak, sh: shoulder.
[b] Area of the peak at lower temperature.

Table 6
HDS and HDN per cent conversion of prepared and commercial catalysts.

	Prepared				Commercial	
	TPA–Ni/SiO_2	MPA–Ni/SiO_2	TPA–Ni/Al_2O_3	MPA–Ni/Al_2O_3	WNi/Al_2O_3	MoNi/Al_2O_3
HDS conversion	19.5	19.8	9.0	14.7	11.0	15.7
HDN conversion	14.3	15.0	12.0	10.7	8.3	8.7

greater activity in hydrotreatment reactions [37]. For HDS reaction, the activity of the catalysts prepared on alumina is smaller than that of the commercial ones. Meanwhile, the activities observed with commercial Mo(W)Ni/alumina catalysts not containing phosphorus (table 6) shows that phosphorus has a greater influence on HDN reaction than on HDS reaction, as previously observed [38]. On the other hand, the catalysts prepared on silica are more HDS and HDN active than the commercial ones.

All the results obtained could be related to the catalyst preparation method because the used precursors (HPA), the support (silica) and the solvent (DMF) are different from those frequently used to prepare the commercial catalysts.

4. Conclusion

The results clearly indicate that the interaction of the heteropolyacids studied is smaller on silica than on alumina. In addition to the fact that the presence of phosphorus plays a role in the NiMo(W)S type I to type II transformation [39], the formation of type II structure, with few or none phase–support bondings, can be favored by the lower interaction. Moreover, the activities are mainly related to the type and to the strength of the HPA interaction with the support. The silica support used in this work is a better carrier than the alumina support for preparing these hydrotreatment catalysts. Even if the use of DMF solution induces the preservation of the Keggin unit on the alumina, the stronger precursor–support interaction lead to the polyoxometallate species well dispersed after the calcination, which can help to the formation of type I structure after sulfurization. So, the use of a precursor–support couple like MPA(TPA)–silica, in which bulk species are found after calcination and a type II structure could be present after sulfurization, gave rise to a higher activity.

Acknowledgement

The authors thank Tcos. L. Osiglio, G. Valle, Lic. D. Peña and Dr. M.G. González for their experimental contribution and the financial support given by Projects PICT0024 (CONICET), PICT97 14-00059-01104 (ANPCyT) and X 224 (UNLP).

References

[1] H. Topsøe, B. Clausen and F. Massoth, in: *Catalysis Science and Technology*, Vol. 11, eds. J.R. Anderson and M. Boudart (Springer, Berlin, 1996).
[2] J.A.R. van Veen, P.A.J.M. Hendriks, R.R. Andrea, E.J.G.M. Romers and A.E. Wilson, J. Phys. Chem. 94 (1990) 5282.
[3] A. Spozhakina, S. Damyanova, V. Sharkova, D. Shopov and T. Yurieva, in: *Proc. VIth Int. Symp. Heterogeneous Catalysis*, Sofia, Bulgaria, Vol. 1 (1987) p. 503.
[4] A. Griboval, P. Blanchard, E. Payen, M. Fournier and J.L. Dubois, Stud. Surf. Sci. Catal. 106 (1997) 181.
[5] A. Spojakina, S. Damyanova, D. Shopov, T.Kh. Shokhireva and T.M. Yurieva, React. Kinet. Catal. Lett. 27 (1985) 333.
[6] A. Griboval, P. Blanchard, L. Gengembre, E. Payen, M. Fournier, J.L. Dubois and J.R. Bernard, J. Catal. 188 (1999) 102.
[7] S. Damyanova, A. Spozhakina and D. Shopov, Appl. Catal. 48 (1989) 177.
[8] A.M. Maitra, N.W. Cant and D.L. Trimm, Appl. Catal. 48 (1989) 187.
[9] C.I. Cabello, I.L. Botto and H.J. Thomas, Appl. Catal. A 197 (2000) 79.
[10] A. Griboval, P. Blanchard, E. Payen, M. Fournier and J.L. Dubois, Catal. Today 45 (1998) 279.
[11] E. Payen, S. Kasztelan and J.B. Moffat, J. Catal. 125 (1990) 45.
[12] G.B. McGarvey and J.B. Moffat, J. Mol. Catal. 69 (1991) 137.
[13] M. Fournier, R. Thouvenot and C. Rocchiccioli-Deltcheff, J. Chem. Soc. Faraday Trans. 87 (1991) 349.
[14] L.R. Pizzio, P.G. Vázquez, M.G. González, M.N. Blanco, C.V. Cáceres and H.J. Thomas, Stud. Surf. Sci. Catal. 106 (1997) 535.
[15] C. Rocchiccioli-Deltcheff and R. Thouvenot, J. Chem. Research (S) (1977) 46.
[16] E. Papaconstantinou, Chem. Soc. Rev. 18 (1989) 1.
[17] K. Nomiya, Y. Sugie, K. Amimoto and M. Miwa, Polyhedron 6 (1987) 519.
[18] P.G. Vázquez, M.G. González, M.N. Blanco and C.V. Cáceres, Stud. Surf. Sci. Catal. 91 (1995) 1121.
[19] R.S. Weber, J. Catal. 151 (1995) 470.
[20] S. Damyanova and J.L.G. Fierro, Appl. Catal. A 144 (1996) 59.
[21] C. Rocchiccioli-Deltcheff, R. Thouvenot and R. Franck, Spectrochim. Acta A 32 (1976) 587.
[22] C. Rocchiccioli-Deltcheff, M. Amirouche, M. Che, J.M. Tatibouët and M. Fournier, J. Catal. 125 (1990) 292.
[23] S. Kasztelan, E. Payen and J.B. Moffat, J. Catal. 125 (1990) 45.
[24] J.B. Mioc, R.Z. Dimitrijevic, M. Davidivic, Z.P. Nedic, M.M. Mitrovic and P.H. Colomban, J. Mater Sci. 29 (1994) 3705.
[25] F. Lefebvre, J. Chem. Soc. Chem. Commun. (1992) 756.
[26] T. Okuhara, N. Mizuno and M. Misono, Adv. Catal. 41 (1996) 130.
[27] J.C. Edwards, C.Y. Thiel, B. Benac and J.F. Knifton, Catal. Lett. 51 (1998) 77.
[28] B.K. Hodnett and J.B. Moffat, J. Catal. 91 (1985) 93.
[29] I.V. Kozhevnikov, A. Sinnema, R.J.J. Jansen and H. van Bekkum, Catal. Lett. 27 (1994) 187.
[30] Y. Izumi, R. Hasebe and K. Urabe, J. Catal. 84 (1983) 402.
[31] P. Dufresne, E. Payen, J. Grimblot and J.P. Bonnelle, J. Phys. Chem. 85 (1981) 2344.
[32] M. Didier, Thesis, Besançon, France (1977).
[33] S. Colque, E. Payen and P. Grange, J. Mat. Chem. 4 (1994) 1343.
[34] E. Payen and S. Kasztelan, Trends Phys. Chem. 4 (1994) 363.
[35] B. Scheffer, N.J.J. Dekker, P.J. Mangnus and J.A. Moulijn, J. Catal. 121 (1990) 31.
[36] J. Laine, J.L. Brito and F. Severino, J. Catal. 131 (1991) 385.
[37] H. Topsøe, R. Candia, N.Y. Topsøe and B.S. Clausen, Bull. Soc. Chim. Belg. 93 (1984) 783.
[38] J.M. Stencel, in: *Raman Spectroscopy in Catalysis*, Catal. Ser., ed. B. Davis (Van Nostrand Reinhold, New York, 1990) p. 62.
[39] S. Eijsbouts, J.N.M. van Gestel, J.A.R. van Veen, V.H.J. de Beer and R. Prins, J. Catal. 131 (1991) 412.